

On line contribution functions and examining spectral line formation in 3D model stellar atmospheres

A. M. Amarsi^{1*}

¹*Mount Stromlo Observatory, Australian National University, Weston Creek, ACT 2611, Australia*

Accepted 2015 June 22. Received 2015 June 13; in original form 2015 February 16

ABSTRACT

Line contribution functions are useful diagnostics for studying spectral line formation in stellar atmospheres. I derive an expression for the contribution function to the absolute flux depression that emerges from three-dimensional ‘box-in-a-star’ model stellar atmospheres. I illustrate the result by comparing the local thermodynamic equilibrium (LTE) spectral line formation of the high-excitation permitted OI 777 nm lines with the non-LTE case.

Key words: line: formation – radiative transfer – methods: numerical – stars: atmospheres

1 INTRODUCTION

The fundamental parameters of stars such as their effective temperature, surface gravity, and chemical composition are not observable quantities: rather, they must be inferred using model stellar atmospheres (Bergemann 2014). Three dimensional (3D) hydrodynamic ‘box-in-a-star’ models (Nordlund 1982) are increasingly being used in this context (Ludwig et al. 2009; Magic et al. 2013a; Trampedach et al. 2013). These present a huge improvement over classical 1D hydrostatic models on account of their ab initio treatment of convective energy transport in the outer envelope that can realistically reproduce the shifting, broadening and strengthening of spectral lines by convective velocity fields and atmospheric inhomogeneities (Nordlund 1980; Asplund et al. 1999). Inferred logarithmic abundances can suffer errors as large as ± 1.0 dex when modelled in 1D (Collet et al. 2008).

Visualizing and understanding spectral line formation in three dimensions is non-trivial. Contribution functions (de Jager 1952; Gurtovenko et al. 1974) are useful tools to that end. They can be interpreted as probability density functions for line formation in the atmosphere (Staude 1972; Magain 1986) and are often used to infer the mean formation depths of spectral lines. The line intensity contribution function (Magain 1986) represents the contribution from different locations of the atmosphere to the depression in the normalized intensity. This quantity is commonly used to study lines in a solar context (Caffau et al. 2008). Since stars are in general not resolved, often more relevant is the line flux contribution function, (Albrow & Cottrell 1996), which is instead formulated in terms of the depression in the absolute flux.

Since all parts of the stellar atmosphere contribute to its observed flux profile, the line flux contribution function is a function of 3D space. Albrow & Cottrell (1996) derive it in the context of 1D model stellar atmospheres, i.e. assuming plane-parallel symmetry. To apply it directly to a 3D model would be to treat the atmosphere as an ensemble of 1D columns i.e. it would be a 1.5D approximation (Kiselman & Nordlund 1995). This is undesirable because the effects of horizontal radiative transfer are entirely neglected. Another approach is to compute the plane-parallel contribution function on a horizontally-averaged, <3D> model. This approach is still not ideal, because it neglects the effects of the atmospheric inhomogeneities which characterize real stellar atmospheres.

In this paper I present in §2 a derivation for the line flux contribution function that is valid in three dimensions. To illustrate the result, I explore in §3 the formation of the high excitation permitted OI 777 nm lines in a 3D hydrodynamic STAGGER model atmosphere (Magic et al. 2013a). I present a short summary in §4.

2 THE 3D LINE FLUX CONTRIBUTION FUNCTION

2.1 Concept

The flux depression at frequency ν from a star of radius R measured by a distant observer is proportional to the total emergent intensity depression,

$$\mathcal{A}_\nu \propto \frac{1}{\pi R^2} \int \int (I_\nu^c - I_\nu) \rho \, d\rho \, d\phi, \quad (1)$$

in the cylindrical polar coordinate system depicted in Figure 1: the polar axis intersects disc-centre and is directed

* E-mail: anish.amarsi@anu.edu.au

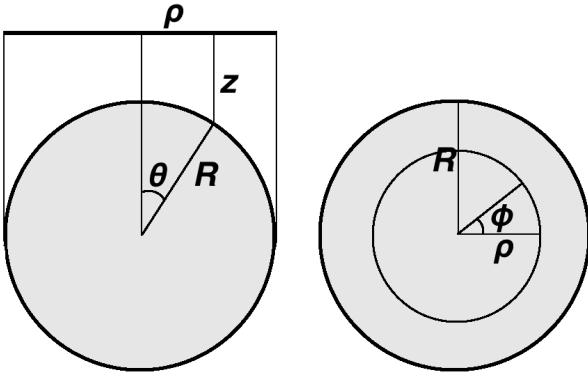


Figure 1. Visual aids to the derivation presented in §2. Left: spherical star and an arbitrary reference plane perpendicular to the observer’s line of sight; the observer is located to the top of the diagram. The spherical polar angle is θ ; conventionally, the notation $\mu = \cos \theta$ is adopted. The cylindrical polar radius is $\rho = R \sin \theta$, where R is the radius of the star. z is the displacement from a point in the atmosphere to the arbitrary reference plane. Right: spherical star as seen by the observer, who is now located out of the page. The azimuthal angle is ϕ . A ring of constant ρ is shown.

towards the observer. I_ν is the specific intensity and I_ν^c is the specific continuum intensity, at some position on the disc, in the direction of the observer. The line flux contribution function \mathcal{C}_ν must satisfy

$$\mathcal{A}_\nu = \int_{\text{box}} \mathcal{C}_\nu(\mathbf{r}) d^3r. \quad (2)$$

Crucially, the integration is not performed over vertical height as in the plane-parallel derivation of [Albrow & Cottrell \(1996\)](#), but over the entire 3D volume in which the line may form. This is the entire volume of the 3D model atmosphere; \mathbf{r} thus specifies a position in this box.

In what follows, equation (1) is manipulated into the form of equation (2), and thereby \mathcal{C}_ν is inferred. The contribution function \mathcal{C} to the integrated line strength $\mathcal{A} = \int \mathcal{A}_\nu d\nu$ is also found, and satisfies $\mathcal{C} = \int \mathcal{C}_\nu d\nu$.

2.2 Derivation

Along any given ray, I_ν and I_ν^c satisfy the respective transport equations,

$$\frac{dI_\nu}{dz} = \alpha_\nu (S_\nu - I_\nu), \quad (3)$$

$$\frac{dI_\nu^c}{dz} = \alpha_\nu^c (S_\nu^c - I_\nu^c), \quad (4)$$

where z is the path distance, increasing upward towards the observer. The linear extinction coefficient α_ν and the source function S_ν are, in terms of their line and continuum components,

$$\alpha_\nu = \alpha_\nu^c + \alpha_\nu^l, \quad (5)$$

$$S_\nu = \frac{\alpha_\nu^c S_\nu^c + \alpha_\nu^l S_\nu^l}{\alpha_\nu} \quad (6)$$

([Hubeny & Mihalas 2014](#)).

Following [Magain \(1986\)](#), an effective transport equation for the intensity depression $D_\nu \equiv I_\nu^c - I_\nu$ is found by

subtracting equation (3) from equation (4),

$$\frac{dD_\nu}{dz} = \alpha_\nu (S_\nu^{\text{eff}} - D_\nu), \quad (7)$$

where the effective source function is

$$S_\nu^{\text{eff}} = \frac{\alpha_\nu^l}{\alpha_\nu} (I_\nu^c - S_\nu^l). \quad (8)$$

In terms of the optical depth along the ray $d\tau_\nu = -\alpha_\nu dz$, equation (7) is expressed as

$$\frac{dD_\nu}{d\tau_\nu} = D_\nu - S_\nu^{\text{eff}}. \quad (9)$$

The formal solution is found by integrating from $\tau_\nu = 0$ to $\tau_\nu \rightarrow \infty$,

$$D_\nu = \int S_\nu^{\text{eff}} e^{-\tau_\nu} d\tau_\nu. \quad (10)$$

Neglecting proportionality factors, the flux depression is obtained by substituting equation (10) into equation (1),

$$\mathcal{A}_\nu = \int \int \int \alpha_\nu S_\nu^{\text{eff}} e^{-\tau_\nu} dz \rho d\rho d\phi, \quad (11)$$

where the integrand is evaluated with the constraint that the emergent rays are directed towards the observer. As the observer is very far from the star, the emergent rays are parallel to each other. Consequently, the last equation is written in terms of an infinitesimal volume element,

$$\mathcal{A}_\nu = \int_{\text{star}} \alpha_\nu S_\nu^{\text{eff}} e^{-\tau_\nu} d^3r. \quad (12)$$

The integration in equation (12) is performed over the entire volume of the star. 3D box-in-a-star models of stellar atmospheres have Cartesian geometry and span a minute surface area of the stars they represent ([Freytag et al. 2012](#); [Magic et al. 2013a](#)). The flux spectrum from the modelled star is (approximately) reproduced by shifting the box tangentially across the spherical surface. This is represented by two integrations: one over the volume of the box and the other over the unit hemisphere. Again neglecting proportionality factors,

$$\mathcal{A}_\nu \approx \int \int_{\text{box}} \alpha_\nu(\mathbf{r}; \Omega) S_\nu^{\text{eff}}(\mathbf{r}; \Omega) e^{-\tau_\nu(\mathbf{r}; \Omega)} d^3r d\Omega, \quad (13)$$

where the functional dependence of the integrand has been made explicit for clarity. The position vector \mathbf{r} specifies a position within the box, and the solid angle Ω specifies the direction of the emergent rays. The infinitesimal solid angle satisfies $d\Omega = d\mu d\phi$, where $\mu = \cos \theta$. After changing the order of integration, the contribution function is inferred to be,

$$\mathcal{C}_\nu(\mathbf{r}) = \int \alpha_\nu(\mathbf{r}; \Omega) S_\nu^{\text{eff}}(\mathbf{r}; \Omega) e^{-\tau_\nu(\mathbf{r}; \Omega)} d\Omega. \quad (14)$$

This represents the contribution of a point within the box to the observed absolute flux depression in the line, at frequency ν . The integrated line strength contribution function follows immediately,

$$\mathcal{C}(\mathbf{r}) = \int \int \alpha_\nu(\mathbf{r}; \Omega) S_\nu^{\text{eff}}(\mathbf{r}; \Omega) e^{-\tau_\nu(\mathbf{r}; \Omega)} d\Omega d\nu. \quad (15)$$

2.3 Rotational broadening

Line broadening caused by the rigid rotation of the star must be included during post-processing. This broadening

will affect the monochromatic quantity \mathcal{A}_ν and hence \mathcal{C}_ν . Following [Dravins & Nordlund \(1990\)](#), the broadened specific intensity is,

$$I_\nu^{\text{broad}} = \mathcal{B}[I_\nu], \quad (16)$$

where \mathcal{B} is a functional which broadens its argument according to,

$$\mathcal{B}[x(v, \theta, \phi)] = \frac{1}{2\pi} \int x(v - V \sin \iota \sin \theta \cos \psi, \theta, \phi) d\psi \quad (17)$$

Here $v = c \frac{\Delta\nu}{\nu}$ is the Doppler speed, V is the rotation speed of the star in the line forming region, ι is the inclination angle of the rotation axis with respect to the observer, and the integral is over an interval of 2π . Retracing the steps above, one obtains a rotationally-broadened contribution function,

$$\mathcal{C}_\nu(\mathbf{r}) = \int \mathcal{B}[\alpha_\nu(\mathbf{r}; \Omega) S_\nu^{\text{eff}}(\mathbf{r}; \Omega) e^{-\tau_\nu(\mathbf{r}; \Omega)}] d\Omega. \quad (18)$$

(In deriving this expression, it is necessary to move \mathcal{B} within the integral of equation (10). This is valid because the atmosphere is assumed to be sufficiently shallow that V does not vary across its depth.)

This integrated line strength \mathcal{A} , should not be affected by the rotation of the star ([Gray 1992](#)). The adopted broadening formalism is consistent with this: integrating equation (17) across the line profile,

$$\int \mathcal{B}[x(v, \theta, \phi)] dv = \int x(v, \theta, \phi) dv, \quad (19)$$

which implies that the contribution function \mathcal{C} is not affected by the rotation of the star.

2.4 Mean formation depth

The interpretation of the contribution function as a probability density function for line formation ([Staude 1972](#); [Magain 1986](#)) suggests a formalism for defining the mean formation value of some quantity q with respect to a line,

$$\mathbb{E}[q] = \frac{\int q(\mathbf{r}) \mathcal{C}(\mathbf{r}) d^3r}{\int \mathcal{C}(\mathbf{r}) d^3r}, \quad (20)$$

and the variance might then be defined in the usual way as $\mathbb{E}[q^2] - \mathbb{E}[q]^2$. For example, $\mathbb{E}[q = \log_{10} \tau_{500}^r]$ may be used to define the mean formation depth, where $\log_{10} \tau_{500}^r$ is the logarithmic radial optical depth at wavelength $\lambda = 500$ nm, a standard measure of depth in stellar atmospheres.

2.5 Relationship to the line flux response function

A related spectral line formation diagnostic is the response function: the linear response of the line to a perturbation in the atmosphere ([Mein 1971](#); [Beckers & Milkey 1975](#); [Caccin et al. 1977](#)). The line flux response function \mathcal{R}_ν must satisfy

$$\delta \mathcal{A}_\nu \equiv \int \mathcal{R}_\nu(\mathbf{r}) \delta \beta(\mathbf{r}) d^3r, \quad (21)$$

where β is an atmospheric parameter (such as temperature).

Following [Magain \(1986\)](#), the response function is obtained by adapting the above derivation. The effective transport equation equation (7) is perturbed so that $D_\nu \rightarrow$

$D_\nu + \delta \beta D_\nu^1$, and the equation for D_ν^1 is solved,

$$\frac{dD_\nu^1}{dz} = \alpha_\nu (S_\nu^{\text{eff},1} - D_\nu^1), \quad (22)$$

where the perturbed effective source function is,

$$S_\nu^{\text{eff},1} = \frac{\partial S_\nu^{\text{eff}}}{\partial \beta} + \frac{1}{\alpha_\nu} \frac{\partial \alpha_\nu}{\partial \beta} (S_\nu^{\text{eff}} - D_\nu). \quad (23)$$

The response function is then found by following the previous derivation, but with D_ν and S_ν^{eff} replaced by D_ν^1 and $S_\nu^{\text{eff},1}$, respectively,

$$\mathcal{R}_\nu(\mathbf{r}) = \int \mathcal{B}[\alpha_\nu(\mathbf{r}; \Omega) S_\nu^{\text{eff},1}(\mathbf{r}; \Omega) e^{-\tau_\nu(\mathbf{r}; \Omega)}] d\Omega, \quad (24)$$

and the response function to the integrated line strength is $\mathcal{R} = \int \mathcal{R}_\nu d\nu$.

Response functions can be used to study the sensitivity of a spectral line to specific atmospheric variables ([Achmad et al. 1991](#)). To identify the line forming regions, however, contribution functions must be used.

2.6 Comparison to the plane-parallel line flux contribution function

In the limit of plane-parallel symmetry, the integrand in equation (14) loses its dependence on the azimuthal angle ϕ : $\alpha_\nu(\mathbf{r}; \Omega) \rightarrow \alpha_\nu(z; \mu)$, $S_\nu^{\text{eff}}(\mathbf{r}; \Omega) \rightarrow S_\nu^{\text{eff}}(z; \mu)$, $\tau_\nu(\mathbf{r}; \Omega) \rightarrow \tau_\nu^r(z; \mu)/\mu$, where z is the geometrical height and τ_ν^r is the radial optical depth. The 3D contribution function \mathcal{C}_ν thus tends to a plane-parallel contribution function $\mathcal{C}_\nu^{\text{pp}}$,

$$\mathcal{C}_\nu^{\text{pp}}(z) = 2\pi \int \alpha_\nu(z; \mu) S_\nu^{\text{eff}}(z; \mu) e^{-\tau_\nu^r(z; \mu)/\mu} d\mu. \quad (25)$$

This expression is the same¹ as that derived by [Albrow & Cottrell \(1996\)](#) in the context of 1D models, i.e. with the implicit assumption of plane-parallel symmetry.

3 EXAMPLE: 3D NON-LTE SPECTRAL LINE FORMATION

The high excitation permitted OI 777 nm lines are known to show departures from local thermodynamic equilibrium (LTE) (LTE; [Sedlmayr 1974](#); [Kiselman & Nordlund 1995](#); [Fabbian et al. 2009](#)). It is interesting to consider how the lines form within the atmosphere when LTE is imposed, and to see what happens once this assumption is relaxed.

To that end, the contribution function \mathcal{C} was implemented into the 3D non-LTE radiative transfer code MULTI3D ([Leenaarts & Carlsson 2009](#)). The contribution function for the OI 777 nm lines was calculated using a model oxygen atom based on those used by [Carlsson & Judge \(1993\)](#), [Kiselman \(1993\)](#) and [Fabbian et al. \(2009\)](#). A temporal snapshot of a 3D hydrodynamic model atmosphere taken from the STAGGER-grid ([Collet et al. 2011](#); [Magic et al. 2013a](#)) was used. The model was of a typical turn-off star, with effective temperature $T_{\text{eff}} \approx 6430$ K, logarithmic surface gravity (in CGS units) $\log_{10} g = 4$, and solar-value

¹ After expressing the contribution function in that paper with respect to geometrical height instead of radial optical depth, they are the same to a factor of 2π , which arises from those authors integrating over spherical polar angle μ instead of solid angle Ω .

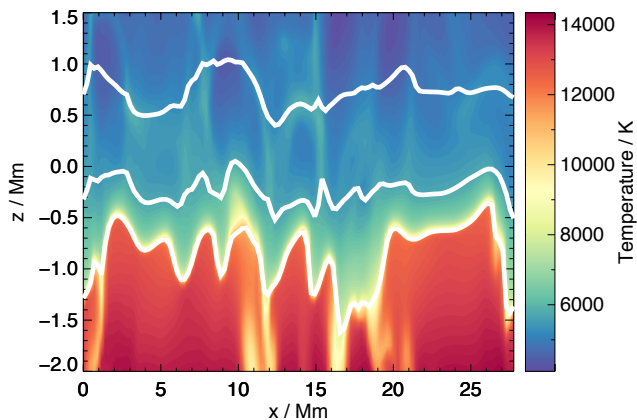


Figure 2. Material temperature in a vertical slice of a temporal snapshot of a 3D hydrodynamic STAGGER model atmosphere (Magic et al. 2013a). The snapshot has effective temperature $T_{\text{eff}} \approx 6430$ K, logarithmic surface gravity (in CGS units) $\log_{10} g = 4$, and solar-value abundances. Contours of standard logarithmic optical depth $\log_{10} \tau_{500}^s = -3, -1, \text{ and } 1$ (from top to bottom) are overdrawn.

abundances (Asplund et al. 2009). The solid angle was sampled using Carlson’s quadrature set A4 (Carlson 1963).

Figure 2 shows the temperature structure in a vertical slice of the snapshot. While the absolute geometrical depth and width scales are arbitrary, zero geometrical depth is roughly located at the photosphere. Just below this depth is the top of the convection zone: hot, light upflows, observed as wide granules, turnover to form cool, dense downflows, observed as narrow intergranular lanes (Magic et al. 2013a). Higher up the atmosphere, reversed granulation patterns can be observed: the material above the hot, light granules expands adiabatically and cools more efficiently, than the material above the intergranular lanes – a detailed discussion can be found in the appendix of Magic et al. (2013b).

The LTE and non-LTE contribution functions in this snapshot slice are shown in Figure 3. They are both normalized such that the maximum value of the non-LTE contribution function is 1.0. The contribution functions reveal that the formation of the lines is qualitatively similar in the two cases. There is no contribution at large optical depths. This can be attributed the attenuation factor $e^{-\tau_\nu}$ in the expression for the contribution function, equation (15): deep within the atmosphere, photons are more likely to be absorbed than to penetrate the atmosphere and reach the observer. Line formation is also inefficient in the optically thin layers. This is by virtue of the line opacity which appears in equation (15): in these layers, $\alpha_\nu^l \approx 0$, so that there is little line absorption. Between these two extremes, line formation becomes possible once the optical depth becomes small, and the factor $I_c - S_l$ appearing in the effective source function becomes non-zero i.e. once the re-emitted light is no longer equal to the absorbed light (Magain 1986; Albrow & Cottrell 1996).

Figure 3 shows that imposing LTE inhibits the forma-

tion of the OI 777 nm lines. Photon losses in the triplet lines themselves (Asplund 2005) drive departures from LTE. The line opacity is larger, and the line source function is smaller, than their LTE counterparts (Fabbian et al. 2009). This leads to a significant strengthening of the lines, correlated with the reversed granulation patterns seen in Figure 2. The equivalent width ratio is $W^{3\text{D non-LTE}}/W^{3\text{D LTE}} \approx 1.5$.

4 SUMMARY

Flux profiles observed from stars have contributions from all parts of its atmosphere: thus, the line flux contribution function is a function of 3D space. In this paper I have shown how to derive the contribution function to the absolute flux depression that emerges from 3D box-in-a-star model stellar atmospheres. The result can be used like other 1D contribution functions (Magain 1986; Albrow & Cottrell 1996) to help one visualize and understand spectral line formation in stellar atmospheres.

ACKNOWLEDGEMENTS

I thank Martin Asplund and Remo Collet for advice on the original manuscript, and Jorrit Leenaarts for providing MULTI3D. This research was undertaken with the assistance of resources from the National Computational Infrastructure (NCI), which is supported by the Australian Government.

References

- Achmad L., de Jager C., Nieuwenhuijzen H., 1991, *A&A*, 250, 445
- Albrow M. D., Cottrell P. L., 1996, *MNRAS*, 278, 337
- Asplund M., 2005, *ARA&A*, 43, 481
- Asplund M., Grevesse N., Sauval A. J., Scott P., 2009, *ARA&A*, 47, 481
- Asplund M., Nordlund Å., Trampedach R., Stein R. F., 1999, *A&A*, 346, L17
- Beckers J. M., Milkey R. W., 1975, *Sol. Phys.*, 43, 289
- Bergemann M., 2014, *Analysis of Stellar Spectra with 3-D and NLTE Models*. Springer International Publishing, pp 187–205
- Caccin B., Gomez M. T., Marmolino C., Severino G., 1977, *A&A*, 54, 227
- Caffau E., Ludwig H.-G., Steffen M., Ayres T. R., Bonifacio P., Cayrel R., Freytag B., Plez B., 2008, *A&A*, 488, 1031
- Carlson B. G., 1963, *Methods in Computational Physics*, 1, 1
- Carlsson M., Judge P. G., 1993, *ApJ*, 402, 344
- Collet R., Asplund M., Trampedach R., 2008, *Mem. Societa Astronomica Ital.*, 79, 649
- Collet R., Magic Z., Asplund M., 2011, *Journal of Physics Conference Series*, 328, 012003
- de Jager C., 1952, *The hydrogen spectrum of the sun*. Druk: Excelsiors Foto-Offset, s-Gravenhage
- Dravins D., Nordlund A., 1990, *A&A*, 228, 203
- Fabbian D., Asplund M., Barklem P. S., Carlsson M., Kiselman D., 2009, *A&A*, 500, 1221
- Freytag B., Steffen M., Ludwig H.-G., Wedemeyer-Böhm S., Schaffenberger W., Steiner O., 2012, *Journal of Computational Physics*, 231, 919
- Gray D. F., 1992, *The observation and analysis of stellar photospheres*. Cambridge Univ. Press, Cambridge
- Gurtovenko E., Ratnikova V., de Jager C., 1974, *Sol. Phys.*, 37, 43

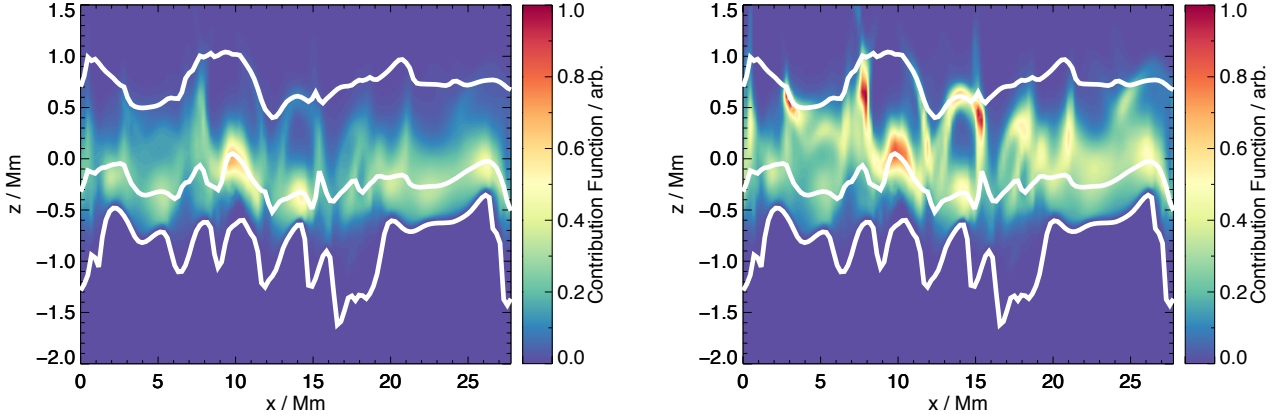


Figure 3. The contribution function $C_L^{b,ox}$ across the oxygen triplet (777.25nm to 777.85nm in vacuum) corresponding to the snapshot slice in Fig. 2, in LTE (left) and in non-LTE (right). These quantities are expressed in the same arbitrary units. Contours of standard logarithmic optical depth $\log_{10} \tau_{500}^r = -3, -1, \text{ and } 1$ (from top to bottom) are overdrawn.

- Hubeny I., Mihalas D., 2014, Theory of Stellar Atmospheres. Princeton Univ. Press, Princeton, NJ
- Kiselman D., 1993, A&A, 275, 269
- Kiselman D., Nordlund A., 1995, A&A, 302, 578
- Leenaarts J., Carlsson M., 2009, in Lites B., Cheung M., Magara T., Mariska J., Reeves K., eds, The Second Hinode Science Meeting: Beyond Discovery-Toward Understanding Vol. 415 of Astronomical Society of the Pacific Conference Series, MULTI3D: A Domain-Decomposed 3D Radiative Transfer Code. p. 87
- Ludwig H.-G., Caffau E., Steffen M., Freytag B., Bonifacio P., Kučinskas A., 2009, Mem. Societa Astronomica Ital., 80, 711
- Magain P., 1986, A&A, 163, 135
- Magic Z., Collet R., Asplund M., Trampedach R., Hayek W., Chiavassa A., Stein R. F., Nordlund Å., 2013a, A&A, 557, A26
- Magic Z., Collet R., Hayek W., Asplund M., 2013b, A&A, 560, A8
- Mein P., 1971, Sol. Phys., 20, 3
- Nordlund A., 1980, in Gray D. F., Linsky J. L., eds, IAU Colloq. 51: Stellar Turbulence Vol. 114 of Lecture Notes in Physics, Berlin Springer Verlag, Numerical simulation of granular convection - Effects on photospheric spectral line profiles. pp 213–224
- Nordlund A., 1982, A&A, 107, 1
- Sedlmayr E., 1974, A&A, 31, 23
- Staude J., 1972, Sol. Phys., 24, 255
- Trampedach R., Asplund M., Collet R., Nordlund Å., Stein R. F., 2013, ApJ, 769, 18